Geophys. J. R. astr. Soc. (1981) 65, 91–101

Telluric measurements and differential geomagnetic soundings in the Rhinegraben (period range: 1–125 s)

Y. Albouy *Orstom, 24, rue Bayard, 75008 Paris, France*

H. Fabriol* *Centre de Recherches Géophysiques, Laboratoire de Géomagnétisme C.N.R.S. 24, rue Lhomond, 75231 Paris, Cedex 05, France*

Received 1980 May 13; in original form 1979 July 31

Summary. In 1976, seven stations measuring the variations of the telluric and geomagnetic fields in the period range 1–125 s were operated in the southern part of the Rhinegraben. The study of the recordings shows that the telluric field is linearly polarized according to a direction perpendicular to that of the horizontal anomalous magnetic fields and that telluric and anomalous magnetic fields have the same time dependence. The conducted currents responsible for the anomaly flow probably into the superficial conductive layer.

Introduction

Recently the Centre de Recherches Géophysiques (CRG) has developed a direct method of characterizing lateral anomalies of conductivity: local differences of the horizontal components of transient geomagnetic variations ΔH and ΔD are measured with respect to a reference station along a profile and studied in the time and frequency domains. The reference station is situated outside the anomaly. At two stations outside an anomaly, differences are zero for uniform source fields.

For each studied anomaly, the most important properties of the anomalous field are the following (Babour *et al.* 1976; Babour & Mosnier 1977):

(a) The anomalous field is linearly polarized and this polarization is independent of time and of the frequency of the variations.

(b) The transformation of the anomalous field from one station to another is a linear transformation which depends only on the situation of the stations and not on time.

Due to the sensors used, these properties have been discovered in the period range from half a minute to a few hours. The aim of this paper is to determine whether these properties are still true for higher frequencies (0.03 to 1 Hz), and to compare the anomalous magnetic field to the telluric field.

*Present address: C'cese Geofisica, PO Box 222, San Ysidro, California 92073, USA.

We have performed two profiles of differential geomagnetic soundings using new equipment. These profiles are the same as those used for slow differential geomagnetic soundings (slow DGS) in the southern part of the graben (Babour & Mosnier 1979) and we have extended the results obtained by the slow DGS to higher frequencies.

Equipment

The magnetic sensors constructed at the CRG are induction coils with a feedback flux; their transfer function is flat in the period range 1–125 s (Clerc, Decriau & Tabbagh 1976) and their noise is less than 12 mγ Hz$^{-1/2}$ (0.012 nT Hz$^{-1/2}$) for a period of 20 s. The telluric field has been measured using Ag–AgCl electrodes (Meunier 1962), the noise of which is less than 0.1 μV Hz$^{-1/2}$ for the same period (Petiau 1976).

In order to restrict the study to the phenomena in the period range 1–125 s, the magnetic and telluric signals have been filtered with the same analogue band-pass filters.

The comparison of the two magnetic sets of equipment has shown that the modulus of their transfer functions is comparable to within 3 per cent, the same result is true for the two telluric sets of equipment. We have three stations equipped with two magnetic and two telluric sensors used to measure the east–west and north–south components of the horizontal transient electromagnetic field. Telluric lines are 200 m long, their orientation and that of the magnetic sensors are undertaken with an accuracy better than 1°.

Two of these stations are mobile and equipped with a telemetric link which enables the transmission in real time of the various signals to the reference station. In this latter station, the various signals are displayed on a graphic chart and recorded on a magnetic tape for later numerical study by computer.

Terminological conventions

$Ex(t)$ and $Ey(t)$ are respectively the north–south and east–west components of the telluric field. The usual unit is the mV km^{-1}.

$H(t)$ and $D(t)$ are respectively the north–south and east–west components of the magnetic field. The usual unit is the γ (nT).

ΔH_{io} and $\Delta D_{io}(t)$ are the instantaneous differences between the components H and D measured at a station i and the same components at the reference o

$$\Delta H_{io}(t) = H_i(t) - H_o(t)$$

$$\Delta D_{io}(t) = D_i(t) - D_o(t).$$

$E(t)$, $\mathscr{H}(t)$ and $\Delta\mathscr{H}(t)$ are respectively the horizontal telluric field, the horizontal magnetic field and the horizontal differential magnetic field.

Fieldwork

The studied area is illustrated in Fig. 1. The dots represent the stations used both by the slow and rapid DGS. The positions of our seven stations are given in the following table (coordinates in grads: note 100 grads = 90°)

Grand Ballon, GBL, reference station	53.22 N	5.30 E
Artzenheim, ART, fixed station	53.47 N	5.78 E
Selestat, SEL, mobile station	53.78 N	5.85 E
Herrlisheim, HER, mobile station	53.31 N	5.55 E
Heisteren, HEI, mobile station	53.29 N	5.83 E
Reiningue, REI, mobile station	53.06 N	5.45 E
Altenberg, ALT, mobile station	52.97 N	5.56 E

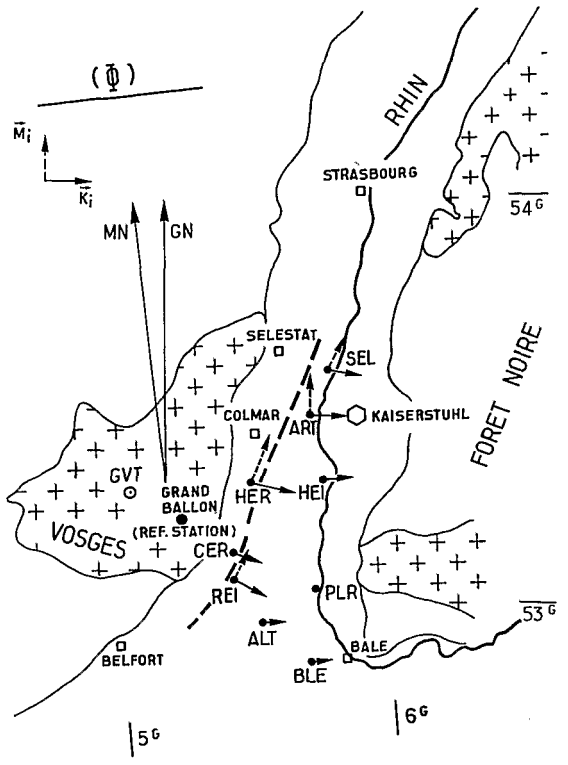

Figure 1. Location of the stations in the Rhinegraben. Φ: induction direction – M_i and K_i: telluric and differential magnetic vectors. (Note coordinates are given in grads: 100 grads = 90°.)

Except Herrlisheim, all these stations were also used by a slow DGS study; Bale (BLE), Cernay (CER) and the 'Grand Ventron' (GVT) were used only by the slow DGS (Babour & Mosnier 1979).

Examples of recordings

We can see, in Fig. 2, simultaneous recording of the two magnetic components, *H* and *D*, at the reference station Grand Ballon (GBL) as well as those of the differential magnetic fields between two mobile stations (SEL and ART) and the reference GBL. We can see also the components of the telluric field simultaneously recorded at SEL and ART.

We point out the following properties:

the magnetic field at the reference station has no particular dominant polarization;
the differential fields are linearly polarized at the other stations;
the moduli of the differential fields are as great as that of the field simultaneously recorded at GBL;
at stations SEL and ART, the telluric field is also linearly polarized.

The properties are illustrated in Fig. 3.

The hodograph of the magnetic field at the reference station does not show any polarization (GBL, Fig. 3f); but on the contrary the differential magnetic field is polarized at both stations (ART, Fig. 3h; SEL, Fig. 3b). The telluric field is also polarized according to a

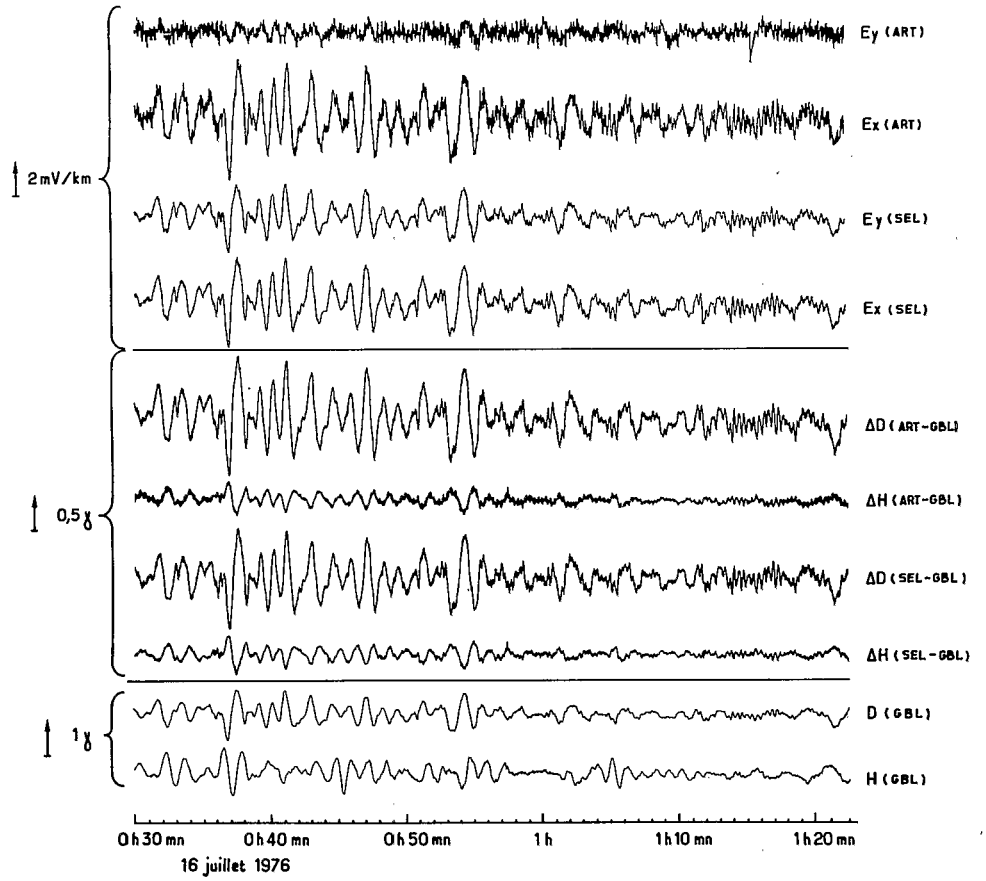

Figure 2. Simultaneous recordings (GBL, ART, SEL) from bottom to top: components of the magnetic field at the reference station (GBL); components of the anomalous magnetic field (ART and SEL); components of the telluric field (ART and SEL).

direction perpendicular to that of the differential magnetic field (ART, Fig. 3g; SEL, Fig. 3a). The north–south components of the telluric field (Ex) are linearly connected from one station to another (ART, SEL; Fig. 3e) and linearly connected to the east–west differential magnetic component (ΔD), (SEL, Fig. 3c; ART, Fig. 3i). All these hodographs correspond to simultaneous pulses of periods from 50 to 80 s; the noise which can be seen on the records is only due to the graphic recorder.

The same remarks can be quoted for all the mobile stations and for shorter periods (down to 8–10 s; beyond this limit the signal/noise ratio is too small). These remarks can be summarized as follows: the law of temporal variations is the same for the horizontal components of the differential field and for the telluric field at one station and from one station to another.

We can write:

$$\Delta H_{io}(t) = K_i \Delta D_{io}(t)$$

$$\Delta D_{io}(t) = L_{ij} \Delta D_{jo}(t)$$

$$Ex_i(t) = M_i Ey_i(t)$$

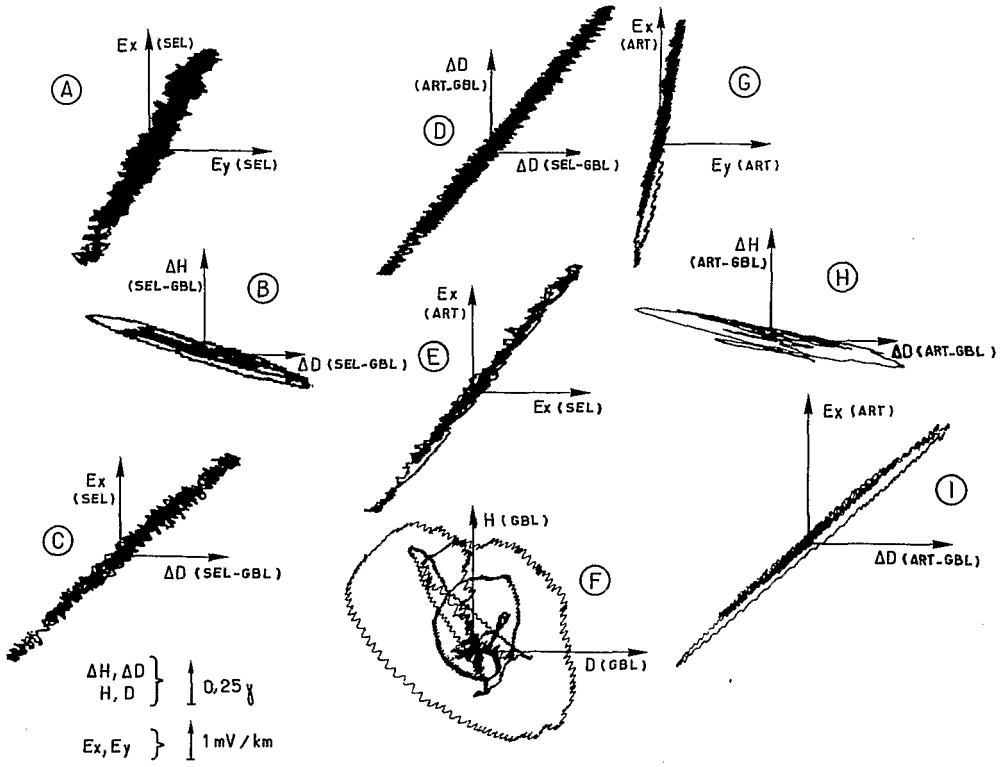

Figure 3. Simultaneous hodographs for periods between 50 and 80 s (GBL, ART, SEL).

$$Ex_i(t) = N_{ij} Ex_j(t)$$

$$Ex_i(t) = O_{ij} D_{jo}(t)$$

K_i, L_{ij}, M_i, N_{ij} and O_{ij} are real.

In order to check these properties in the frequency domain, we have calculated the transfer functions, linking Ex_i to Ey_i, ΔD_i to Ex_i, Ex_i to Ex_{ART} and ΔH_i to ΔH_{ART} (Schmucker 1973). The imaginary parts of the transfer function are very small, i.e. there is no appreciable difference of phase shift between any two components. We have also computed the coherencies (the coherency between $X(t)$ and $Y(t)$ being defined by $C_{xy} = |S_{xy}|/(S_{xx} \cdot S_{yy})^{1/2}$, S_{xy} being the cross-spectrum and S_{xx}, S_{yy} the autospectrum). All the coherencies are larger than 0.85 and vary by no more than 10 per cent for the different recordings.

Hence, the horizontal differential magnetic field $\Delta\mathscr{H}$ can be written as the product of a time function and a vectorial spatial function (Babour & Mosnier 1977):

$$\overrightarrow{\Delta\mathscr{H}}(i, t) = \overrightarrow{\mathbf{h}(i)} \cdot R(t), \tag{1}$$

similarly for the telluric field

$$\overrightarrow{\mathbf{E}(i, t)} = \overrightarrow{\mathbf{e}(i)} \cdot R(t). \tag{2}$$

It appears, from these relations, that the study of this anomaly can be split into two parts: the study of the geometry of the anomaly (**h**, **e**), and that of the temporal dependence $R(t)$.

Study of the geometry of the anomaly $(h(i), e(i))$

Using (1), we have normalized the differential geomagnetic fields using ART as normalization station and defined a vector $\vec{K}_i$ by its north–south (K_{hi}) and east–west (K_{di}) components:

$$K_{hi} = \Delta H_{io}(\Delta H^2_{\mathrm{ART-GBL}} + \Delta D^2_{\mathrm{ART-GBL}})^{-1/2}$$

$$K_{di} = \Delta D_{io}(\Delta H^2_{\mathrm{ART-GBL}} + \Delta D^2_{\mathrm{ART-GBL}})^{-1/2}.$$

This vector, independent of the time, is proportional to the anomalous field in each station i.

We have found that, down to short periods (10 s), the vectors K_i are the same as those derived by the slow DGS (Babour & Mosnier 1979). We must note that the largest vector is obtained at station HER, which was not occupied by slow DGS.

We have also computed normalized telluric vectors using ART as the normalization station:

$$M_{xi} = E_{xi}(Ex^2_{\mathrm{ART}} + Ey^2_{\mathrm{ART}})^{-1/2}$$

$$M_{yi} = E_{yi}(Ex^2_{\mathrm{ART}} + Ey^2_{\mathrm{ART}})^{-1/2}.$$

These two vectors K_i and M_i are independent of time and are proportional to the anomalous magnetic and telluric fields respectively.

We have illustrated K_i and M_i in Fig. 1. Telluric and differential magnetic fields are found to be parallel and perpendicular respectively to the axis of the maximum of the anomaly (dashed line).

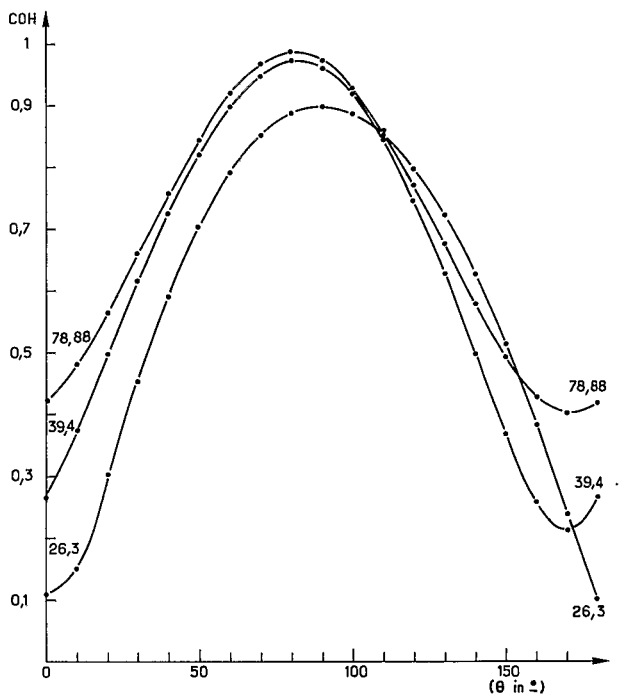

Figure 4. Coherencies versus θ, between ΔD(ART) and $\mathscr{H}$(GBL) projected on the direction θ for three different periods (26.3–39.4–78.88 s);

Study of the temporal dependence

(a) INDUCTION DIRECTION

The slow DGS has shown that the anomalous magnetic field is excited by the normal magnetic field projected in a direction varying from 120° for periods of 2 hr to 80° for periods of 10 min. This direction is the preferential induction direction (Vasseur *et al.* 1977). In order to know this direction for shorter periods, we have computed it for various periods between 120 and 10 s.

With this in view, we have calculated the coherency between the component ΔD of the anomalous field and the normal field projected on the direction θ (with respect to north).

Fig. 4 presents the variation of the modulus of the coherencies versus θ obtained at station ART for various periods. These variations point out the existence of maxima which depend slightly on the period of the phenomena. These directions are 80° (78 s) and 90° (shorter periods; ΔD is linked only to D). Taking into account the weak variation of this direction in our period range we will take in the sequel 80° for induction direction, represented by Φ on Fig. 1.

(b) TRANSFER FUNCTION

In order to know the frequency dependence of the anomaly, we have computed the transfer function between ΔD at the various stations and the normal horizontal magnetic field projected in the direction most effective for induction (80°).

$$\Delta D_i(f) = G(f) \cdot (H_0(f) \cos\theta + D_0(f) \sin\theta).$$

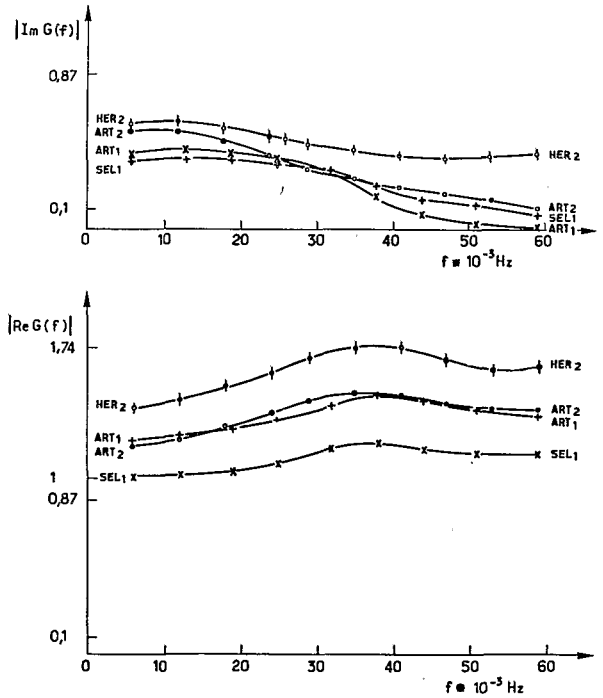

Figure 5. Imaginary and real values of different $G(f)$ (HER, ART and SEL). $G(f)$ is the transfer function linking ΔD, obtained at each station, to the normal field (GBL) projected on the induction direction $\theta = 80°$.

Fig. 5 presents the real and imaginary part of $G(f)$ for periods between 100 and 15 s for various stations and for two samples of the same station (ART). One can note on this figure that all the transfer functions have a similar shape. This proportionality is the expression in the frequency domain of the relation (1) observed in the time domain.

The results obtained at station ART from two samples lead to an identical transfer function, this gives an indication of the accuracy of the calculation.

It can also be noticed that the real part of the transfer functions presents a maximum for frequencies of $30-40 \times 10^{-3}$ Hz (25–33 s).

We have obtained similar transfer functions at stations situated 40 km apart (HER, SEL) and the Rhinegraben has a very different structure for these stations. So we have to consider that the currents which create the anomalous field at these two stations are the same and that these currents are not locally induced but channelled in the Rhinegraben.

We will try, in the next section, to estimate the parts of the currents locally induced with respect to the total currents which flow in this area.

(c) CONDUCTION AND INDUCTION CURRENTS

To estimate the normal telluric component, we shall use the relations of the magnetotelluric method (MT).

Reddy & Rankin (1972), Rooney & Hutton (1977) interpreted MT curves, obtained respectively in the plains of Alberta and in the Kenyan rift, using a two-dimensional model. They show clearly that, on a superficial conductive layer and at a sufficient distance from the resistive edge, $\rho_{\parallel}$ curves (E-polarization) are close to ρ_{1D} curves (one-dimensional) for short periods.

The resistivity log obtained near Herrlisheim (HER) is displayed in Fig. 6. This station located at 6 km from the resistive Vosges, on a conductive layer (depth: 0.1 km, thickness: 1 km), can be compared to the Canadian stations; at HER, the skin depths of the periods used in the conductive layer would be comprised between 3.3 and 7.5 km whereas the skin depths for the Canadian survey would be between 1.3 and 40 km. So we can calculate $E_{(\omega)}/H_{(\omega)}$ ratios by the mean of the classical one-dimensional formulations of the magnetotelluric method.

Let us consider one particular period near the centre of our period range: 34 s.

The calculated E/H ratio is equal to 1.66.

Along a direction $\alpha = 20^{\circ}$ N, direction of the axis of anomaly, (E-polarization) the corresponding measured ratios are:

$$|E_{\mathrm{HER},\,\alpha}|/|\mathscr{H}_{\mathrm{GBL},\,\alpha+\pi/2}| = 6.80$$

$$|\Delta\mathscr{H}_{\mathrm{HER\cdot GBL},\,\alpha+\pi/2}|/|\mathscr{H}_{\mathrm{GBL},\,\alpha+\pi/2}| = 1.41.$$

The ratios are the modulus of transfer functions linking telluric and differential magnetic components to the normal magnetic component.

We can write, for the telluric and magnetic fields, that the measured components are equal to the normal components – which would be recorded without a geomagnetic anomaly – plus the components of the anomalous field. For instance:

$$E_{\alpha} = E_{\mathrm{n},\alpha} + E_{\mathrm{a},\alpha}$$

(n: normal, a: anomalous).

For a normal field equal to 1 nT, the anomalous telluric field is

$$E_{\mathrm{a}} = 6.80 - 1.66 = 5.14 \text{ mV km}^{-1}.$$

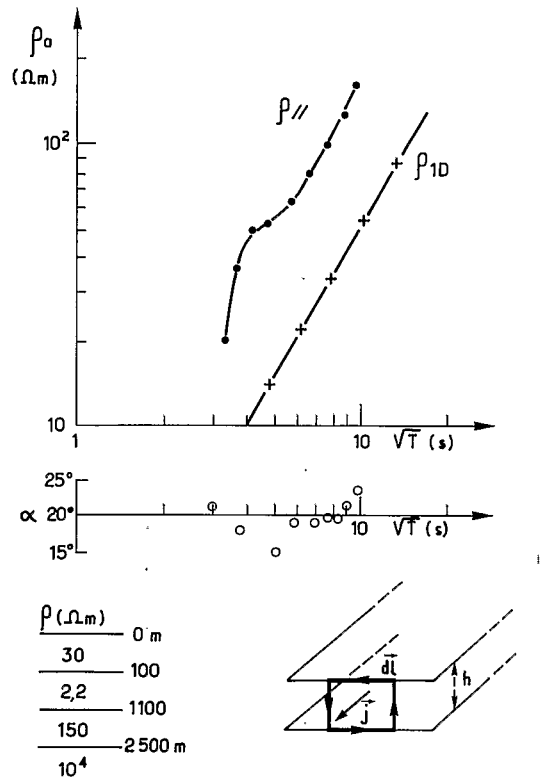

Figure 6. From bottom to top: resistivity log at HER and pattern of flowing currents in the conductive layer; principal direction of the impedance tensor versus periods; observed and theoretical MT curves at HER: $\rho_{\parallel}$ and ρ_{1D}.

The anomalous telluric field in the direction of 20° N is almost 4 times larger than the normal field.

With conduction currents we can write:

$\vec{\mathbf{E}} = \rho \cdot \vec{\mathbf{J}}$ (J: current density).

If we assume that all the conduction currents are flowing in the highly conductive layer (e = 1000 m, ρ = 2.2 ohm m) we may write:

$|\mathbf{E}_a|_{\mathrm{mV\,km^{-1}}} = 2.2 \cdot 10^{+6} |\mathbf{J}|_{\mathrm{A\,m^{-2}}}$.

The corresponding anomalous component may be calculated roughly if we suppose the conductive layer unlimited in the two horizontal directions (Fig. 6).

$$\oint |\Delta \mathscr{H}| \cdot \mathbf{d}l = \iint |\mathbf{J}| \cdot ds$$

$$2|\Delta \mathscr{H}| \cdot dl = |\mathbf{J}| \cdot h \cdot dl \qquad (|\Delta \mathscr{H}| \text{ in A m}^{-1}).$$

$$|\Delta \mathscr{H}| = 200\pi \cdot (|\mathbf{E}_a|/\rho) \cdot h \times 10^{-6}$$

($|\Delta \mathscr{H}|$ in nT, $|\mathbf{E}_a|$ in mV km^{-1}, h in m, ρ in Ω m)

$|\Delta \mathscr{H}| = 1.47$ nT.

The modulus of computed ΔH is not very different from the observed value (1.41 nT^{-1}).

An analogous result can be obtained by taking all the sedimentary layers into account instead of the highly conductive alone. The integrated resistivity $\Sigma e_i/\Sigma(e_{i/\rho i})$ is equal to 4.5 ohm m and $h = \Sigma e_i = 2500$ m. We obtain: $|\Delta \mathscr{H}| = 1.50$ nT.

Hence, the anomalous magnetic field may be explained by currents flowing in the highly conductive layer or in the sedimentary layers.

The normal telluric field is weak in comparison with the field of the conducted currents (from 1 to almost 4 in our example). There is an important enhancement of the telluric field, above these highly conductive zones, consequently any investigation by telluric currents is invalid in these zones. There is also an enhancement of the E/H ratio: the telluric field increases more than the magnetic field and the magnetotelluric curves are also wrong in the same range of periods. In the area being studied, this enhancement certainly modifies the estimation of the thickness of the conductive layer and the resistivity of the resistive layers; in fact we do not know down to which period this phenomenon exists; it is possible that for frequencies higher than 0.1 Hz only induced currents exist and that MT curves are right. To point out the difference between measured and calculated MT curves, Fig. 6 shows the theoretical apparent resistivity ρ_{1D} and the resistivity $\rho_{\parallel}$ ($\alpha = 20°$).

Conclusions

Many authors have studied the Rhinegraben using induction techniques.

Winter (1972) calculated transfer functions linking anomalous fields to normal fields but for periods larger than 10 min, Scheelke (1972) and Haak & Reitmayr (1974) have performed several profiles using telluric and magnetotelluric methods.

These authors calculated the impedance tensor, its principal direction and the two corresponding resistivities ($\rho_{\parallel}$ and $\rho_{\perp}$). Scheelke used a two-dimensional model for interpretation of MT curves. Our own results are, in part, in good agreement with those obtained by the above cited authors: the $\rho_{\parallel}$ and α curves (Fig. 6) agree well with the curves given by Scheelke for stations having comparable locations.

Moreover we think that the two-dimensional model used by Scheelke cannot explain the physical properties described in this paper.

$\Delta \mathscr{H}$ and E have a time and space dependence naturally separated, hence the phase of $\Delta \mathscr{H}$ and E are independent of the position of the station in the anomalous area.

E_a may be 4 times larger than E_n, $\Delta \mathscr{H}$ 1.5 times larger than $\mathscr{H}$.

In order to explain these experimental results, we must consider three-dimensional models, with conduction currents, like those of Vasseur & Weidelt (1977) and Lajoie & West (1976), but these models cannot yet be applied to obtain accurate results on the scale of the graben. All these authors point out the channelling phenomenon which has to be taken into account in the interpretation of the conductivity anomalies such as those of the Rhinegraben.

Acknowledgments

This work has been supported by the EEC (contract 08076 EGF) and partly by the INAC, through the ATP 'Transfert d'énergie à traverse l'écorce terrestre'.

References

Babour, K. & Mosnier, J., 1977. Differential geomagnetic sounding, *Geophysics*, 42, 66–76.

Babour, K. & Mosnier, J., 1979. Differential geomagnetic sounding in the Rhinegraben, *Geophys. J. R. astr. Soc.*, 58, 135–144.

Babour, K., Mosnier, J., Daignieres, M., Vasseur, G., Le Mouel, J. L. & Rossignol, J. C., 1976. A geomagnetic variation anomaly in the northern Pyrenees, *Geophys. J. R. astr. Soc.*, **45**, 583–600.

Clerc, G., Decriau, J. P. & Tabbagh, J., 1976. Caracterisation en bruit de capteurs magnetometriques dans la gamme de 1 mha à 1 hz, *Note Centre Rech. géophys.*, Garchy, Nièvre, CMD 03-1976.

Haak, V. & Reitmayr, G., 1974. The distribution of electrical resistivity in the Rhinegraben area as determined by telluric and magnetotelluric methods, in *Approaches to Taphrogenesis*, pp. 366–369, eds Illies, J. H. & Fuchs, K., Schweizerbart, Stuttgart.

Lajoie, J. J. & West, G. F., 1976. The electromagnetic response of a conductive inhomogeneity in a layered earth, *Geophysics*, **31**, 1133–1156.

Meunier, J., 1962. Contribution à l'étude expérimentale des problèmes d'enregistrement électrotelluriques et à l'amélioration des techniques de prospection, *thèse de 3é cycle*, Faculté des Sciences, Paris.

Petiau, G., 1976. Etude spectrale du bruit et de diverses causes de perturbation affectant l'enregistrement du champ tellurique de 0.01 à 100 hz, *Note Centre Rech. géophys.*, Garchy, Nièvre, CRG MTT 10.

Reddy, T. K. & Rankin, D., 1972. On the interpretation of the magnetotelluric data in the plains of Alberta, *Can. J. Earth Sci.*, **9**, 514–527.

Rooney, D. & Hutton, V. R. S., 1977. A magnetotelluric and magnetovariational study of the Gregory Rift Valley, Kenya, *Geophys. J. R. astr. Soc.*, **51**, 91–119.

Scheelke, I., 1972. Magnetotellurische messungen im Rheingraben und ihre Deutung mit zweidimensionalen modellen, *Diss. Techn.*, University of Braunschweig.

Schmucker, U., 1973. Regional induction studies: a review of methods and results, *Phys. Earth planet. Int.*, **7**, 365–378.

Vasseur, G., Babour, K., Menvielle, M. & Rossignol, J. C., 1977. The geomagnetic variation anomaly in the northern Pyrenees: study of the temporal variation, *Geophys. J. R. astr. Soc.*, **49**, 593–607.

Vasseur, G. & Weidelt, P., 1977. Bimodal electromagnetic induction in non-uniform thin sheets with an application to the Pyrenean induction anomaly, *Geophys. J. R. astr. Soc.*, **51**, 669–690.

Winter, R., 1972. A model of the resistivity distribution from geomagnetic depth sounding, in *Approaches to Taphrogenesis*, pp. 369–375, eds Illies, J. H. & Fuchs, K., Schweizerbart, Stuttgart.